Nondestructive Measurements of Complex Tensor Permittivity of Anisotropic Materials Using a Waveguide Probe System

Chih-Wei Chang, *Member, IEEE,* Kun-Mu Chen, *Fellow, IEEE,* and Jian Qian, *Member, IEEE*

Abstract— **A nondestructive measurement of electromagnetic (EM) properties of anisotropic materials using an open-ended waveguide probe has been conducted. Two coupled electric field integral equations (EFIE's) for the aperture electric field are derived and solved numerically by employing the method of moments (MoM). After the determination of the aperture electric field, the reflection coefficient of the incident wave can be expressed in terms of the EM parameters of the material. Then, the EM parameters of the material layer can be inversely determined if the reflection coefficient of the incident wave is experimentally measured. A series of experiments has been conducted using the waveguide probe system constructed at MSU electromagnetics laboratory. The inverse results of the EM properties of various materials are presented. Finally, the effects of material parameters on the probe input admittance that cause problems in the measurement are analyzed.**

I. Introduction

Due to the rapid advance in material manufacturing, an increasing demand has emerged for accurate nondestructive measurements of the material parameters, especially for anisotropic fiber-reinforced composites. Techniques for the measurement of the material EM properties have been developed by numerous investigators using various methods. Some researchers employed an open-ended coaxial probe [1]–[12], while others used an open-ended waveguide probe [13]–[14]. However, all of them were limited to the measurement of the EM parameters of isotropic materials.

In this paper, a nondestructive measurement of EM properties of anisotropic materials using an flanged open-ended waveguide probe is conducted. We solve the problem directly by matching boundary conditions at discontinuity interfaces to constitute two coupled integral equations for the unknown aperture electric field. We assume that the total electric field in the probe aperture includes not only a dominant TE_{10} mode but also infinite higher-order modes. The EM field excited in the waveguide is expressed based on the Hertzian potentials, while the EM fields in the material layer and the free space backing the material layer are derived based on the concept of eigenmodes of the spectrum-domain transverse EM fields. After the EFIE's are formulated, the method of moments (MoM) is employed to convert the EFIE's to a matrix equation, and the aperture electric field can then be accurately determined by solving the matrix equation. Once the determination of the aperture electric field is found, relevant quantities such as the reflection coefficient of the incident dominant wave and the probe input admittance can be expressed as functions of material parameters.

A series of experiments was conducted to measure the reflection coefficient or the input admittance of the waveguide probe system, which is constructed with a flanged, open-ended X-band waveguide, using a vector network analyzer (HP-8720B). The Newton-Raphson method is then used to inversely determine the EM parameters of the material from the measured probe input admittance. For a layer of anisotropic material with a diagonal form of the complex tensor permittivity, three measurements are required to determine the three unknown principal permittivities.

Manuscript received September 14, 1995; revised March 20, 1996. This work was supported in part by Boeing Defense and Space Group under Contract B-225383 and a Research Excellence Fund from the State of Michigan.
C.-W. Chang and K.-M. Chen are with the Department of Electrical Engineering, Michigan State University, East Lansing, MI 48824 USA.
J. Qian is with the Department of Electronic Science and Engineering, Nanjing University, Nanjing, 210008 PRC.
Publisher Item Identifier S 0018-9480(96)04724-2.

II. Problem Description and EFIE's

The geometry to be studied is shown in Fig. 1 where a flanged open-ended rectangular waveguide is placed against a layer of unknown anisotropic material of thickness d backed by free space. Inside the waveguide region, a dominant TE_{10} mode of field is excited and it propagates toward the probe aperture. In addition to the reflected TE_{10} mode, higher order modes of fields are excited near the aperture due to the discontinuity between the waveguide and the material slab. The electromagnetic wave carried by the waveguide radiates into the material layer and through the open space backing it. If the electromagnetic fields in the material layer and the open space are established based on Maxwell's equations, the problem can be solved by matching the fields at the waveguide-material and the material-air interfaces.

Assuming a suppressed $e^{j\omega t}$ harmonic time dependence of the fields, the transverse EM fields excited inside the waveguide region can be derived as [15]

$$\vec{E}_t = j\omega\mu(\hat{z} \times \nabla_t)\Pi_h + \nabla_t \frac{\partial}{\partial z}\Pi_e \quad (1)$$

$$\vec{H}_t = \nabla_t \frac{\partial}{\partial z}\Pi_h - j\omega\mu(\hat{z} \times \nabla_t)\Pi_e \quad (2)$$

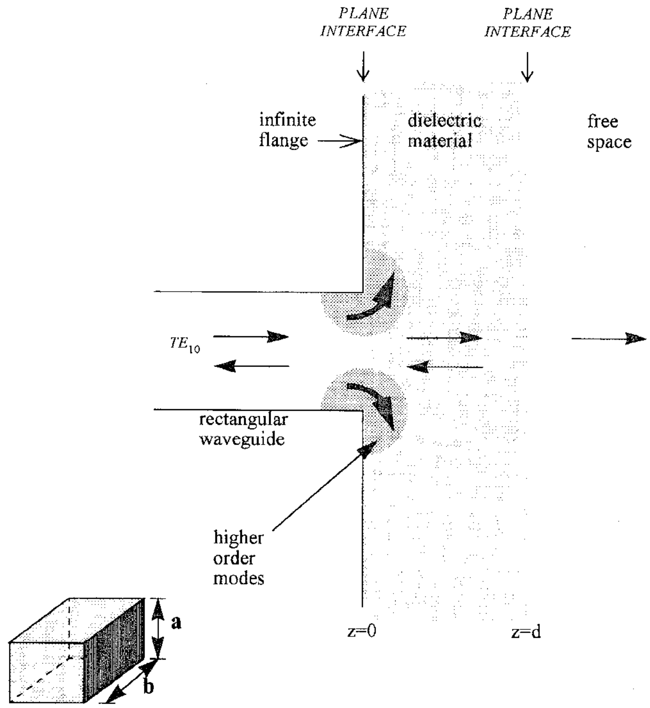

Fig. 1. The arrangement of nondestructive measurement using a waveguide probe system.

where

$$\Pi_h = a_{10}\cos\left(\frac{\pi x}{a}\right)(e^{-\Gamma_{10}z} + \mathrm{R}e^{\Gamma_{10}z}) + \sum_n\sum_m A_{nm}\cos\left(\frac{n\pi x}{a}\right)\cos\left(\frac{m\pi y}{b}\right)e^{\Gamma_{nm}z} \quad (3)$$

is the magnetic type Hertzian potential with $n, m = 0, 1, 2, \cdots$ and n and m cannot be both equal to zero

$$\Pi_e = \sum_n\sum_m B_{nm}\sin\left(\frac{n\pi x}{a}\right)\sin\left(\frac{m\pi y}{b}\right)e^{\Gamma_{nm}z} \quad (4)$$

is the electric type Hertzian potential with $n, m = 1, 2, \cdots$; and

$$\Gamma_{nm} = \sqrt{\left(\frac{n\pi}{a}\right)^2 + \left(\frac{m\pi}{b}\right)^2 - k_0^2}. \quad (5)$$

Note that a_{10}, A_{nm} and B_{nm} represent the amplitude of the dominant TE_{10} mode, and the unknown TE and TM higher order modes, respectively; R denotes the reflection coefficient of the incident dominant mode; and $Re(\Gamma_{nm}) \geq 0$ and $Im(\Gamma_{nm}) \geq 0$ are required, for all values of n and m.

The fields external to the waveguide aperture are formulated directly from Maxwell equations. In an anisotropic space with a complex tensor permittivity of the form

$$\bar{\bar{\epsilon}} = \begin{bmatrix} \epsilon_{xx} & \epsilon_{xy} & 0 \\ \epsilon_{yx} & \epsilon_{yy} & 0 \\ 0 & 0 & \epsilon_z \end{bmatrix} \quad (6)$$

the resulting six scalar component equations of $\nabla \times \vec{E} = -j\omega\mu_0\vec{H}$ and $\nabla \times \vec{H} = j\omega\bar{\bar{\epsilon}} \cdot \vec{E}$ can be reduced to a matrix equation for the spectrum-domain transverse EM fields as [16]

$$\frac{d}{dz}\tilde{T} = \bar{\bar{S}} \cdot \tilde{T} \quad (7)$$

where

$$\tilde{T} \equiv (\tilde{E}_x, \tilde{E}_y, \eta_0\tilde{H}_x, \eta_0\tilde{H}_y)^T \quad (8)$$

with $\eta_0 = 120\pi$, and

$$\bar{\bar{S}} \equiv -\begin{bmatrix} 0 & 0 & a & b \\ 0 & 0 & c & d \\ \alpha & \beta & 0 & 0 \\ \gamma & \delta & 0 & 0 \end{bmatrix} \quad (9)$$

$$\begin{bmatrix} a & b \\ c & d \end{bmatrix} \equiv \frac{j}{\omega\epsilon_z\eta_0}\begin{bmatrix} k_xk_y & \omega^2\mu_0\epsilon_z - k_x^2 \\ -\omega^2\mu_0\epsilon_z + k_y^2 & -k_xk_y \end{bmatrix} \quad (10)$$

$$\begin{bmatrix} \alpha & \beta \\ \gamma & \delta \end{bmatrix} \equiv \frac{j\eta_0}{\omega\mu_0}\begin{bmatrix} -\omega^2\mu_0\epsilon_{yx} - k_xk_y & -\omega^2\mu_0\epsilon_{yy} + k_x^2 \\ \omega^2\mu_0\epsilon_{xx} - k_y^2 & \omega^2\mu_0\epsilon_{xy} + k_xk_y \end{bmatrix}. \quad (11)$$

Therefore, the vector of the spectrum-domain transverse EM fields in the anisotropic material layer can be expressed as

$$\tilde{T} = \sum_{m=1}^{4} A_m\vec{v}_m e^{\lambda_m z} \quad (12)$$

where A_m denotes the unknown coefficient of the mth eigenvector, $\vec{v}_m$, which with a corresponding eigenvalue λ_m satisfies the relation $\bar{\bar{S}} \cdot \vec{v}_m = \lambda_m\vec{v}_m$. Similarly, the spectrum-domain transverse EM fields in the free space backing the material layer are derived as a degenerate eigenvalue problem of (7) and they are expressed as

$$[\tilde{E}_{xa}, \tilde{E}_{ya}, \eta_0\tilde{H}_{xa}, \eta_0\tilde{H}_{ya}]^T = B_2\vec{v}_{2a}e^{-\lambda_a(z-d)} + B_4\vec{v}_{4a}e^{-\lambda_a(z-d)} \quad (13)$$

where B_2 and B_4 represent the unknown coefficients of the forward propagating waves characterized by the same eigenvalue, λ_a, and two different eigenvectors, $\vec{v}_{2a}$ and $\vec{v}_{4a}$, respectively.

Applying the boundary conditions at $z = d$ and substituting unknown coefficients A_3 and A_4 in terms of A_1 and A_2 lead (12) to [17]

$$\tilde{T} = A_1(\vec{v}_1e^{\lambda_1 z} + r_1\vec{v}_3e^{\lambda_3 z} + r_3\vec{v}_4e^{\lambda_4 z}) + A_2(\vec{v}_2e^{\lambda_2 z} + r_2\vec{v}_3e^{\lambda_3 z} + r_4\vec{v}_4e^{\lambda_4 z}). \quad (14)$$

If we further simplify the expression of (14) at the waveguide aperture with notations of

$$[C_1, C_3, D_1, D_3]^T = (\vec{v}_1e^{\lambda_1 z} + r_1\vec{v}_3e^{\lambda_3 z} + r_3\vec{v}_4e^{\lambda_4 z})\mid_{z=0} \quad (15)$$

$$[C_2, C_4, D_2, D_4]^T = (\vec{v}_2e^{\lambda_2 z} + r_2\vec{v}_3e^{\lambda_3 z} + r_4\vec{v}_4e^{\lambda_4 z})\mid_{z=0}. \quad (16)$$

the unknown coefficients A_1 and A_2 can then be expressed in terms of the aperture electric field by using the orthogonality properties. Substituting A_1 and A_2 into (14) allows the transverse aperture magnetic fields in the material side to be expressed as

$$H_x\,|_{z=0^+}=\frac{j}{\omega\mu}\int_{-\infty}^{\infty}\int_{-\infty}^{\infty}e^{jk_xx}e^{jk_yy}\left[M_y(k_x,\,k_y)\iint E_{xo}^e + N_y(k_x,\,k_y)\iint E_{yo}^e\right]dk_x\,dk_y \quad (17)$$

$$H_y\,|_{z=0^+}=\frac{-j}{\omega\mu}\int_{-\infty}^{\infty}\int_{-\infty}^{\infty}e^{jk_xx}e^{jk_yy}\left[N_x(k_y,\,k_x)\iint E_{xo}^e + M_x(k_y,\,k_x)\iint E_{yo}^e\right]dk_x\,dk_y \quad (18)$$

where

$$\iint E_{xo}^e \equiv \int_0^b\int_0^a E_{xo}e^{-jk_xx}e^{-jk_yy}\,dx\,dy,$$
$$\iint E_{yo}^e \equiv \int_0^b\int_0^a E_{yo}e^{-jk_xx}e^{-jk_yy}\,dx\,dy \quad (19)$$

and

$$M_y(k_x,\,k_y)\equiv\frac{\omega\mu}{j\eta_0(2\pi)^2}\frac{C_4D_1-C_3D_2}{C_1C_4-C_2C_3},$$
$$N_y(k_x,\,k_y)\equiv\frac{\omega\mu}{j\eta_0(2\pi)^2}\frac{C_1D_2-C_2D_1}{C_1C_4-C_2C_3}$$
$$N_x(k_x,\,k_y)\equiv\frac{\omega\mu}{j\eta_0(2\pi)^2}\frac{C_3D_4-C_4D_3}{C_1C_4-C_2C_3},$$
$$M_x(k_x,\,k_y)\equiv\frac{\omega\mu}{j\eta_0(2\pi)^2}\frac{C_2D_3-C_1D_4}{C_1C_4-C_2C_3}. \quad (20)$$

With a similar technique, the aperture electric field can be derived from (1) in terms of the amplitudes a_{10}, A_{nm} and B_{nm}; and then these amplitudes can be inversely expressed in terms of the aperture electric field by using the orthogonality properties [18]. Consequently the substitution of these amplitudes in the aperture magnetic field derived from (2) leads to the transverse aperture magnetic fields in the waveguide side as

$$H_x\,|_{z=0^-}=\frac{j}{\omega\mu_0}\Bigg\{C\sin\left(\frac{\pi x}{a}\right)-C_{10}\sin\left(\frac{\pi x}{a}\right)\cdot\int_0^b\int_0^a E_{yo}\sin\left(\frac{\pi x'}{a}\right)dx'\,dy' - \sum_n\sum_m\sin\left(\frac{n\pi x}{a}\right)\cos\left(\frac{m\pi y}{b}\right)\cdot\left[C_{yx}(n,\,m)\iint E_{xo}+C_{yy}(n,\,m)\iint E_{yo}\right]\Bigg\} \quad (21)$$

$$H_y\,|_{z=0^-}=\frac{j}{\omega\mu_0}\sum_n\sum_m\cos\left(\frac{n\pi x}{a}\right)\sin\left(\frac{m\pi y}{b}\right)\cdot\left[C_{xx}(n,\,m)\iint E_{xo}+C_{xy}(n,\,m)\iint E_{yo}\right] \quad (22)$$

where

$$\iint E_{xo}\equiv\int_0^b\int_0^a E_{xo}\cos\left(\frac{n\pi x}{a}\right)\sin\left(\frac{m\pi y}{a}\right)dx\,dy \quad (23)$$

$$\iint E_{yo}\equiv\int_0^b\int_0^a E_{yo}\sin\left(\frac{n\pi x}{a}\right)\cos\left(\frac{m\pi y}{b}\right)dx\,dy \quad (24)$$

and

$$C\equiv -j\frac{2\pi}{a}\omega\mu_0\Gamma_{10}$$
$$C_{10}\equiv\frac{2\Gamma_{10}}{ab}$$
$$C_{xx}(n,\,m)\equiv\frac{-4\epsilon_{nm}}{ab\Gamma_{nm}}\left[k_0^2-\left(\frac{m\pi}{b}\right)^2\right]$$
$$C_{xy}(n,\,m)\equiv\frac{-4\epsilon_{nm}}{ab\Gamma_{nm}}\left(\frac{n\pi}{a}\right)\left(\frac{m\pi}{b}\right)$$
$$C_{yx}(n,\,m)\equiv C_{xy}(n,\,m)$$
$$C_{yy}(n,\,m)\equiv\frac{-4\epsilon_{nm}}{ab\Gamma_{nm}}\left[k_0^2-\left(\frac{n\pi}{a}\right)^2\right]. \quad (25)$$

In addition, the relationship between the reflection coefficient R and the aperture electric field E_{yo} is given as

$$R=\left(\frac{2/-j\omega\mu_0}{a_{10}b\pi}\int_0^b\int_0^a E_{yo}\sin\left(\frac{\pi x}{a}\right)dx\,dy\right)-1. \quad (26)$$

Matching the tangential magnetic fields across the aperture $z=0$ leads to two coupled integral equations for the aperture electric field as follows:

$$\sum_n\sum_m\left(\frac{\mu}{\mu_0}\right)\cos\left(\frac{n\pi x}{a}\right)\sin\left(\frac{m\pi y}{b}\right)\cdot\left[C_{xx}(n,\,m)\iint E_{xo}+C_{xy}(n,\,m)\iint E_{yo}\right]+\int_{-\infty}^{\infty}\int_{-\infty}^{\infty}e^{jk_xx}e^{jk_yy}\left[N_x(k_y,\,k_x)\iint E_{xo}^e+M_x(k_y,\,k_x)\iint E_{yo}^e\right]dk_xdk_y=0 \quad (27)$$

$$\sum_n\sum_m\left(\frac{\mu}{\mu_0}\right)\sin\left(\frac{n\pi x}{a}\right)\cos\left(\frac{m\pi y}{b}\right)\cdot\left[C_{yx}(n,\,m)\iint E_{xo}+C_{yy}(n,\,m)\iint E_{yo}\right]+\int_{-\infty}^{\infty}\int_{-\infty}^{\infty}e^{jk_xx}e^{jk_yy}\left[M_y(k_x,\,k_y)\iint E_{xo}^e+N_y(k_x,\,k_y)\iint E_{yo}^e\right]dk_x\,dk_y+C_{10}\left(\frac{\mu}{\mu_0}\right)\sin\left(\frac{\pi x}{a}\right)\int_0^b\int_0^a E_{yo}\sin\left(\frac{\pi x'}{a}\right)dx'\,dy'=C\left(\frac{\mu}{\mu_0}\right)\sin\left(\frac{\pi x}{a}\right). \quad (28)$$

These EFIE's are key functions to be used for the further development.

III. Numerical Calculation and Results

The EFIE's for the unknown aperture electric field are solved by the Method of Moments [19]. The unknown aperture electric field components are first expanded into a set of appropriately chosen basis functions $\{e_\beta(x, y)\}$ as follows:

$$E_{xo}(x, y) = \sum_\beta a_\beta e_\beta^x(x, y) \tag{29}$$

$$E_{yo}(x, y) = \sum_\beta b_\beta e_\beta^y(x, y) \tag{30}$$

where the eigenmodes of the waveguide are chosen as the basis functions. In addition, Galerkin's technique is used to convert the EFIE's to a matrix equation as

$$\begin{bmatrix} D_{\alpha\beta}^{xx} & D_{\alpha\beta}^{xy} \\ D_{\alpha\beta}^{yx} & D_{\alpha\beta}^{yy} \end{bmatrix} \begin{bmatrix} a_\beta \\ b_\beta \end{bmatrix} = \begin{bmatrix} 0 \\ F_\alpha \end{bmatrix} \tag{31}$$

which can be solved by a numerical program for the unknown expansion amplitudes a_β and b_β of the aperture electric field components. The evaluation of matrix elements is discussed in detail in [17] and the numerical results comparing with the existing results are presented to verify the accuracy of this technique, as well as the validity of the computer program.

Fig. 2 shows the input admittances of a waveguide probe when the probe is placed against a layer of quartz with a dielectric constant of $\epsilon_r = 3.76$ and a thickness of 3.3 mm. Our results are compared to the theoretical and experimental results of Croswell *et al.* [20] where they only considered a dominant TE_{10} mode in their theoretical calculation. These figures show that our numerical results compare quite well with the theoretical value of [20] when only a dominant mode is considered in the calculation. However, when higher order TE and TM modes are taken into account, our numerical results match very well with their experimental results, much better than their theoretical results do. This phenomenon has also been pointed out by many researchers [10], [21] that a good convergence can be obtained with a dominant mode plus three higher order modes (TE_{30}, TE_{12} and TM_{12}) in case of dealing with isotropic materials.

To check the convergence of our numerical algorithm for the case of anisotropic materials, we calculated the input impedance of the probe as a function of frequency when it is placed at 0 degree orientation angle against a layer of anisotropic material with assumed permittivities of $\epsilon_1 = 5.4-j0.3$, $\epsilon_2 = 5.8-j0.4$ and $\epsilon_3 = 3.8-j1.7$, and an assumed thickness of 2.8 mm. The calculated probe input impedance is shown in Fig. 3. In this figure, we observe that accurate results on the input impedance can be obtained using only the dominant TE_{10} mode for the probe aperture field; the inclusion of higher order modes in the probe aperture field does not improve the probe input impedance. This may indicate that for the measurement of anisotropic materials, higher order modes of the probe aperture field do not cause significant effects. This phenomenon deviates from that observed in the case of isotropic material as shown in Fig. 2.

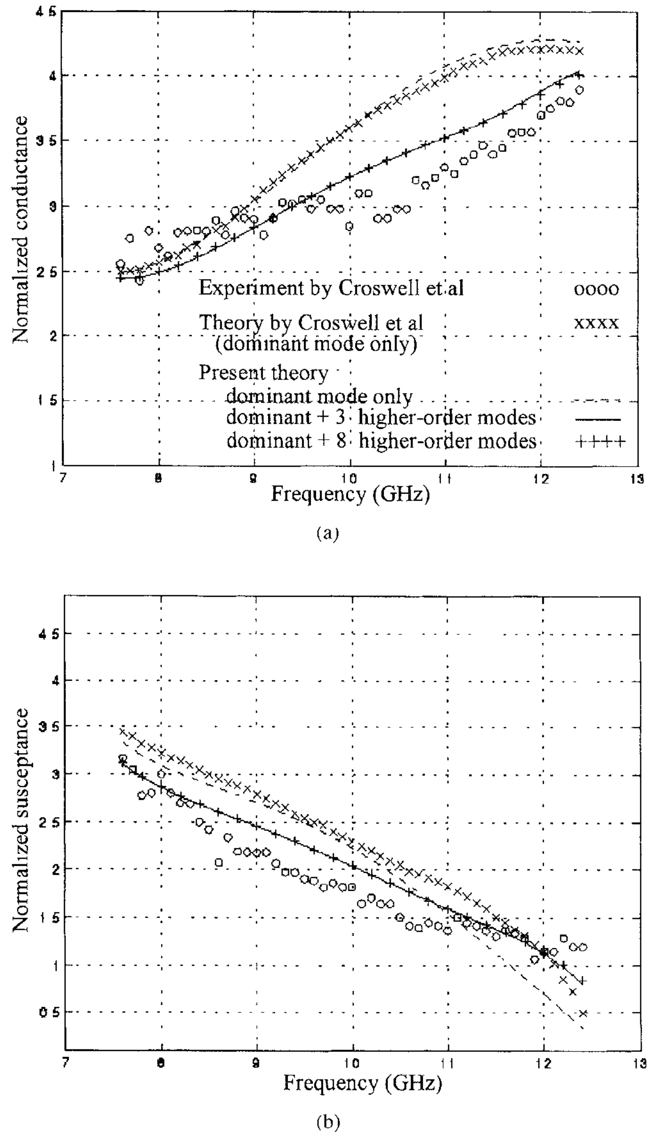

Fig 2 Comparison of probe input admittances as a function of frequency with theoretical and experimental results of Croswell *et al.* [20]. (Quartz $\mathrm{Re}(\epsilon_r) = 3.76$, thickness = 3.3 mm).

IV. Experimental Measurements

A waveguide probe system consisting of an X-band open-ended rectangular waveguide with cross-sectional dimensions of 10.16 mm by 22.86 mm terminated on a 46 cm by 46 cm metal flange for measuring the complex permittivity of isotropic and anisotropic materials has been constructed at MSU electromagnetics laboratory. A vector network analyzer (HP 8720B) is connected to the waveguide probe and it excites a dominant TE_{10} mode in the waveguide in the frequency range of 8 GHz to 12 GHz.

The reflection coefficient at the probe aperture is automatically measured and recorded with the network analyzer. As shown in Fig. 4, the equivalent two-port network between the probe aperture and the measurement reference plane of the network analyzer can be characterized by an $[S]$ matrix. According to [22]–[23], the scattering $[S]$ parameters of the equivalent network can be determined via a calibration procedure which employs three reference measurements (typically uses offset short circuits). With these $[S]$ parameters, the measured reflection coefficient at the reference plane of a network analyzer can be converted to the reflection coefficient at the probe aperture.

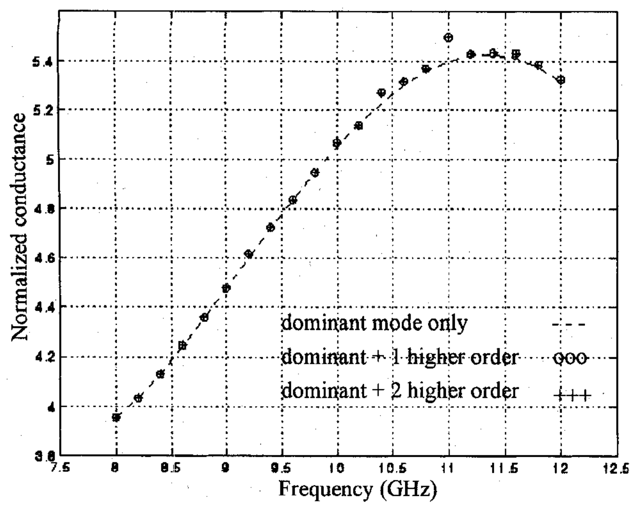

(a)

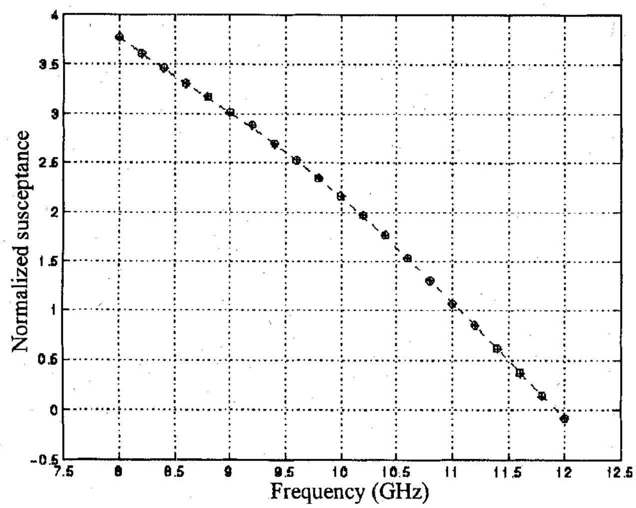

(b)

Fig. 3. Probe input admittance (theoretical) as a function of frequency when the probe is placed against a known anisotropic material layer.

After the probe reflection coefficient is measured, an inversion technique based on Newton's iterative method [24] is introduced. Newton's method, an extension of the Newton-Raphson method, is well known to have a key relationship of

$$\vec{x}_{k+1} = \vec{x}_k - (J_k)^{-1} F_k. \tag{32}$$

For example, if we use Newton's method to solve three equations for three unknowns simultaneously, we define

$$F(\vec{x}) = \begin{bmatrix} f_1(x_1, x_2, x_3) \\ f_2(x_1, x_2, x_3) \\ f_3(x_1, x_2, x_3) \end{bmatrix} \tag{33}$$

$$\vec{x} = [x_1 x_2 x_3]^T \tag{34}$$

and

$$(J)_{i,j} = \frac{\partial f_i(\vec{x})}{\partial x_j}, \qquad 1 \le i, j \le 3. \tag{35}$$

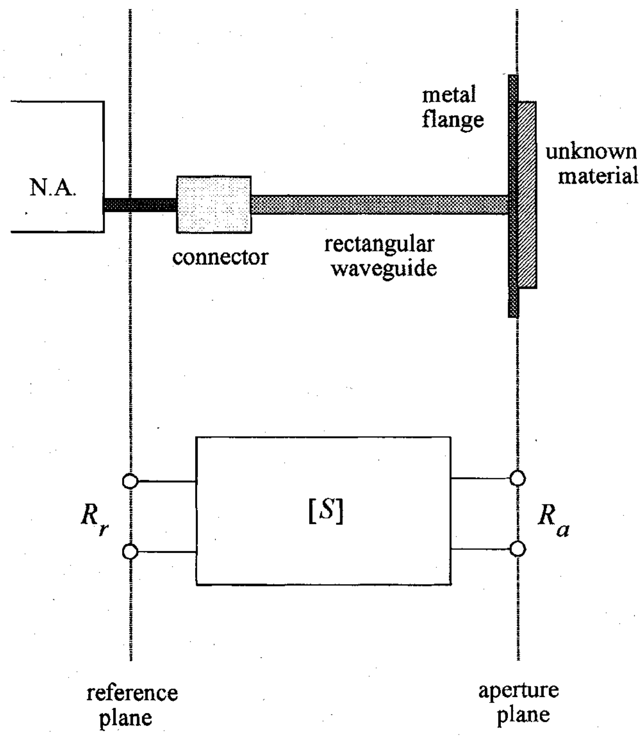

Fig. 4. Representation of the equivalent two-port network between the waveguide aperture and the measurement reference plane of a network analyzer.

For our problem

$$F(\vec{x}) = \vec{R}_{th}(\vec{x}) - \vec{R}_m \tag{36}$$

where $\vec{R}_m(\vec{x})$ represents three different measured reflection coefficients or input impedances of the probe at three different probe orientations with respect to the material principal axis, and $\vec{R}_{th}(\vec{x})$ represents the three corresponding theoretical probe reflection coefficients or input impedances calculated with a set of $\vec{x}$ representing three diagonal components of the material tensor permittivity. The iterative process of (32) can be started with an initial guessed values of $\vec{x}$ and the final solutions of $\vec{x}_{k+1}$, after $(k+1)^{th}$ iteration, will be reached when $F(\vec{x}_{k+1}) \approx 0$ is satisfied at some preset accuracy. The final solutions of $\vec{x}_{k+1}$ are the inversely determined tensor permittivities of the measured material sample.

A series of experiments was conducted on both isotropic and anisotropic material layers. The measured results of the dielectric constant for some known materials, such as air and teflon slab, were first obtained as shown in Fig. 5 to verify the technique and the results were found to be quite accurate.

The measured complex tensor permittivities of a sample of anisotropic material supplied by the Composite Material Laboratory of Michigan State University, are shown in Fig. 6. This sample is a six ply unidirectional glass-fiber/epoxy matrix with a thickness of 2.8 mm. In the figure, there are two sets of results; the solid lines represent the measured permittivities obtained by employing three different measurements of the probe input admittances with the probe orientations of 0, 45, and 90 degrees with respect to a principal axis of the material, and the dashed lines represent data with the probe

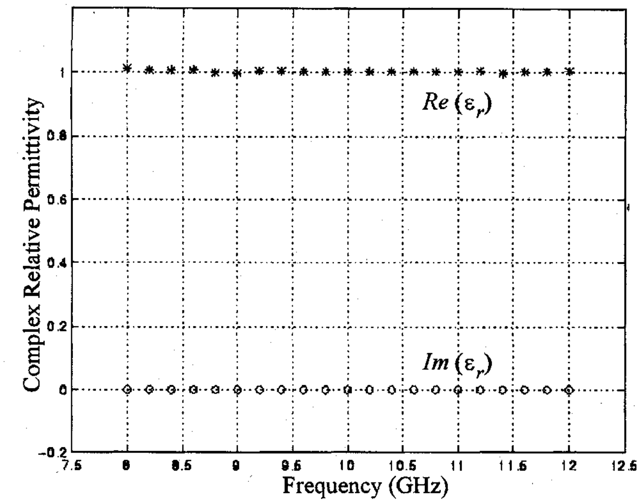

(a)

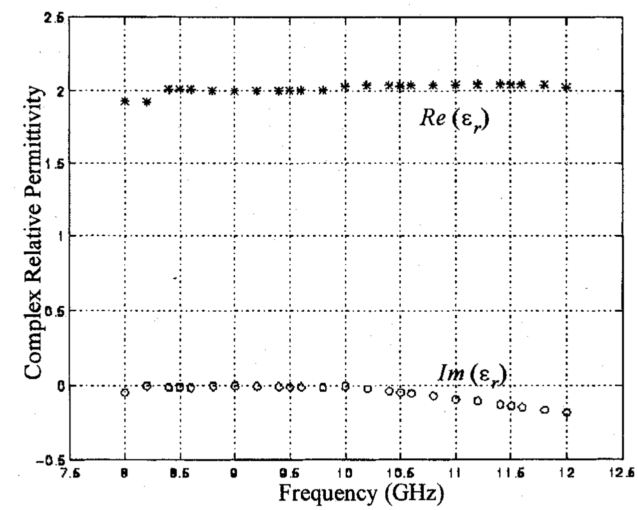

(b)

Fig. 5. Measured complex relative permittivities of (a) air and (b) Teflon, $\epsilon_r = 2.046$.

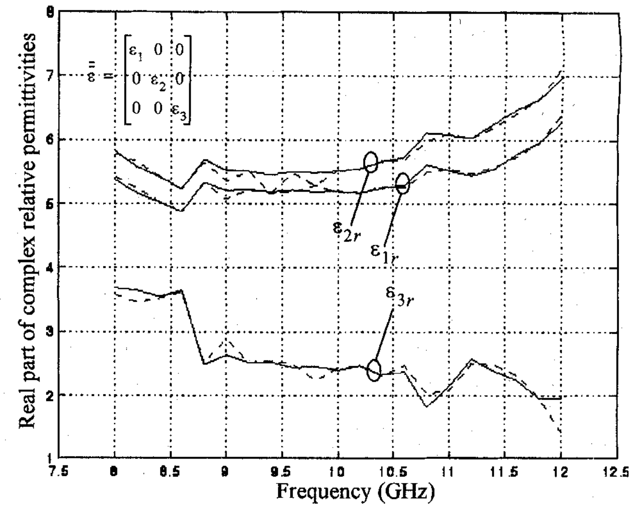

(a)

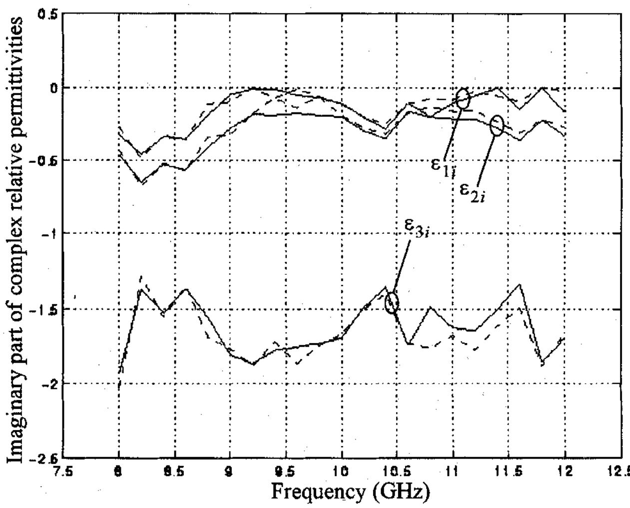

(b)

Fig. 6. Measured complex tensor permittivities of an anisotropic material layer (glass-fiber/epoxy) with a thickness of 2.8 mm. The solid lines represent the inverse results by employing measurements with probe orientations of 0, 45, and 90 degrees with respect to a principal axis of the material, while the dashed lines represent the corresponding results with 0, 30, and 90 degrees.

orientations of 0, 30, and 90 degrees. Both cases give quite consistent results for the real and imaginary components of the permittivities. The accuracy of the measured results is satisfactory because the results are consistent with empirically estimated values.

Fig. 7 shows the measured complex tensor permittivities of a sample of anisotropic material, manufactured by Boeing Airplane Company with a thickness of 1.35 mm. This material sample is made of 20 layers of dielectric fiber/epoxy mat and the dielectric fiber consists of 98% polyesther and 2% carbon with a length of 3/4 inch and a very thin diameter. The fibers are directed in a such a way that it presents some degree of anisotropic property. The results are determined inversely by employing three measurements of the probe input admittances with the probe orientations of 0, 30, and 90 degrees with respect to a principal axis of the material. In the figure, we only show the real and imaginary components of the principal permittivities in the transverse directions, while the permittivity in the perpendicular direction is omitted because it is found to be highly unstable giving a value between 10 to 10 000 for both real and imaginary components. The difficulty encountered in this case can be explained by an analysis of effects of EM parameters on the probe input admittance.

V. Analysis

To determine the effects of EM parameters on the probe input admittance, we developed the following scheme. Let's assume that a waveguide probe is placed against an anisotropic material layer with three principal complex permittivities of $\epsilon_1 = 5.4 - j5.3$, $\epsilon_2 = 5.8 - j6.4$ and $\epsilon_3 = 3.8 - j5.7$. For this kind of material, we can first plot the probe input admittance as a function of the material thickness. If we further change one of the imaginary components of three principal permittivities in the calculation, the effects of the specific

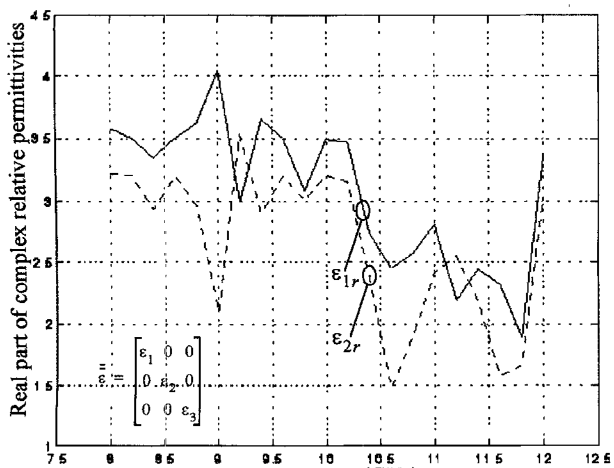

(a)

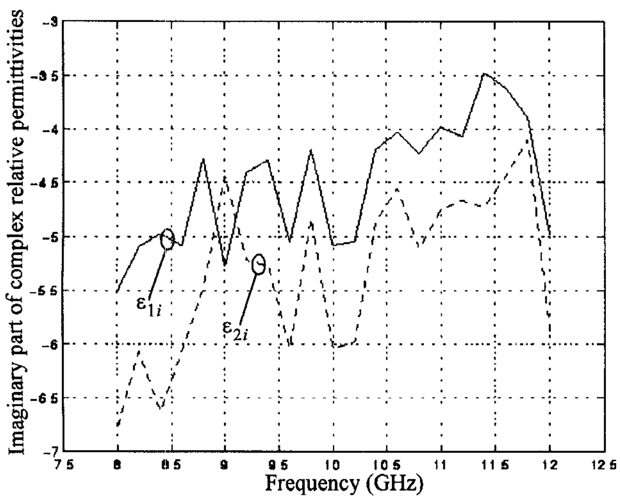

(b)

Fig. 7. Measured tensor permittivities of an anisotropic material layer (dielectric-fiber/epoxy) with a thickness of 1.35 mm. The results were determined inversely by employing measurements with probe orientations of 0, 30, and 90 degrees with respect to a principal axis of the material. The complex permittivity in the direction perpendicular to the waveguide aperture was determined to be unstable and is omitted here.

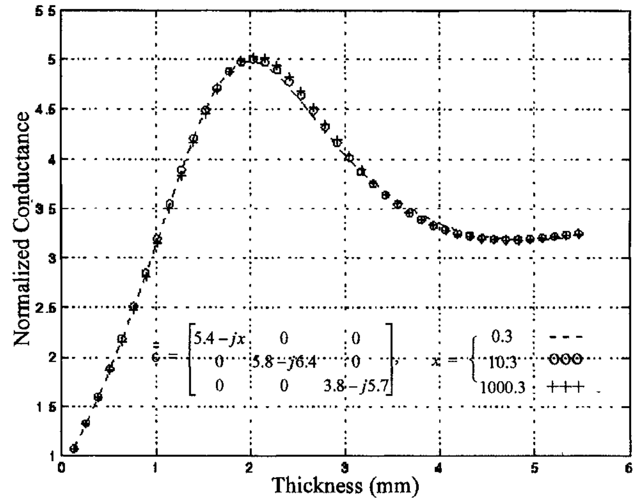

(a)

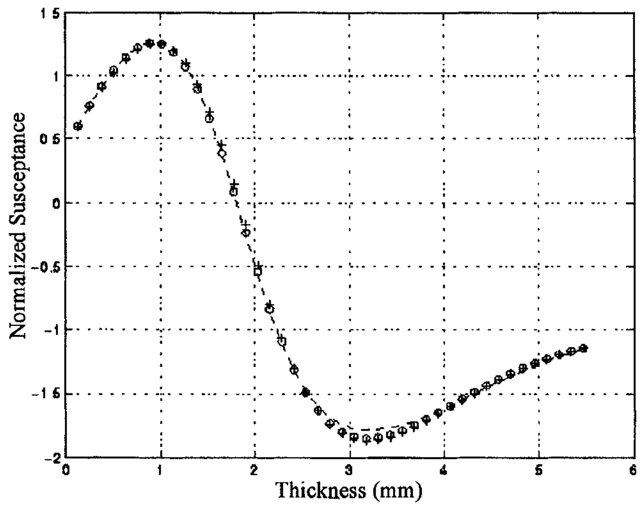

(b)

Fig. 8. Theoretical probe input admittances as a function of the material thickness at 10 GHz when the probe is placed against an anisotropic material layer with assumed permittivities and various conductivities in the x direction.

conductivity associated with the thickness on the probe input admittance can then be sought.

Fig. 8 shows the theoretical probe input admittance at 10 GHz as a function of the material thickness when the material conductivity in the x direction is varied. Since the aperture electric field is dominated by the dominant TE_{10} mode which has an electric field in the y direction only, changing the material conductivity in the x direction does not change the induced current in the material layer, leading to an insignificant change in the probe input admittance. This phenomenon can be verified from the figure that shows almost identical curves for the three different conductivities in the x direction.

At the same frequency, Fig. 9 shows the theoretical probe input admittance of a waveguide probe as a function of the material thickness when the material conductivity in the y direction is varied. Since the electric field of the dominant TE_{10} mode is in the y direction, the change in the material conductivity in the y direction should cause a great change in the probe input admittance. We can observe that the probe input admittances for three different conductivities are highly distinguishable over a range of material thickness. It is also noted that when the measured anisotropic material is highly conductive in the y direction, the probe input admittance becomes independent of the material thickness because the material layer essentially becomes a short circuit.

Similarly, Fig. 10 shows the theoretical probe input admittance of a waveguide probe as a function of the material thickness when the material conductivity in the z direction is varied. We found that when the anisotropic material is highly conductive in the direction perpendicular to the waveguide aperture, the probe input admittance is nearly independent of the conductivity in the z direction when the material thickness is smaller than 1.75 mm. This phenomenon is probably due to the fact that the induced current in the perpendicular direction

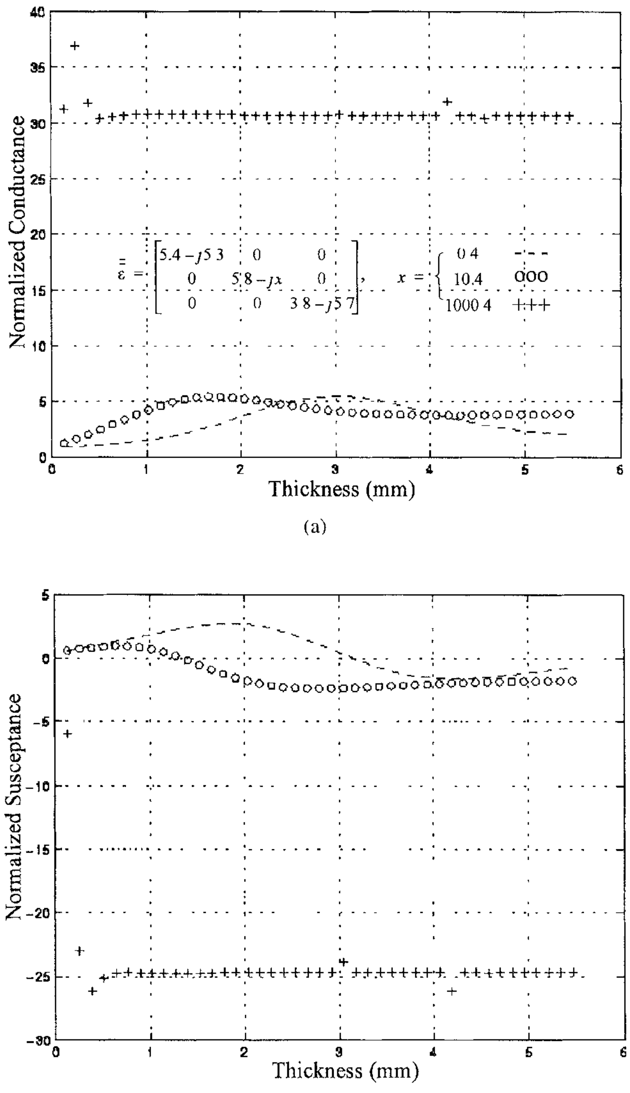

Fig. 9. Theoretical probe input admittance as a function of the material thickness at 10 GHz when the probe is placed against an anisotropic material layer with assumed permittivities and various conductivities in the y direction

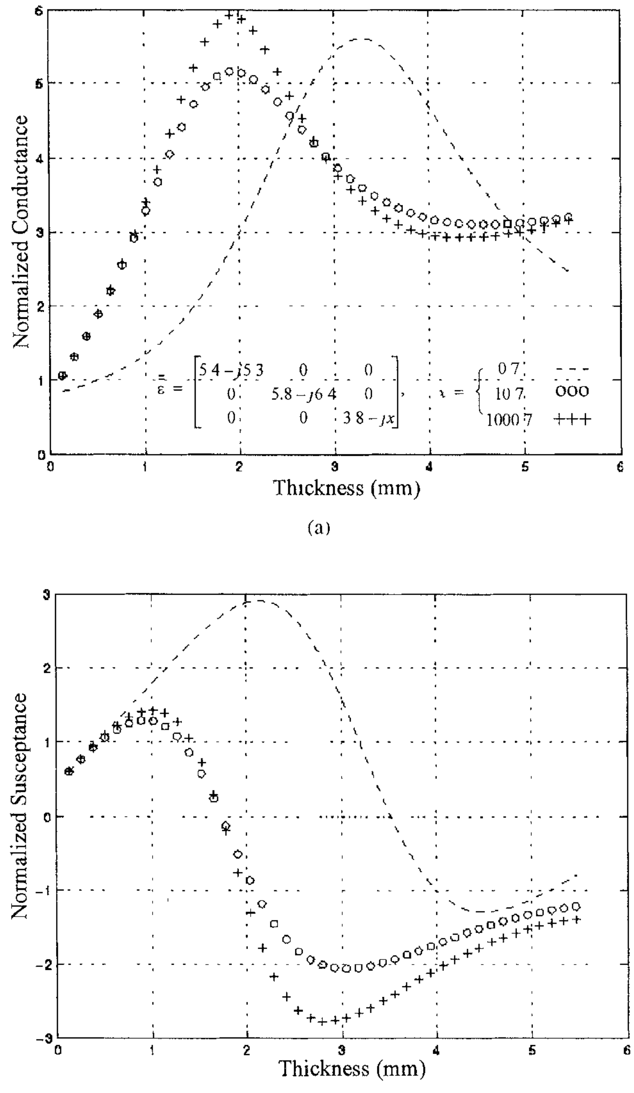

Fig. 10. Theoretical probe input admittance as a function of the material thickness at 10 GHz when the probe is placed against an anisotropic material layer with assumed permittivities and various conductivities in the z direction

of a thin conducting layer is quite small and is independent of the conductivity in the perpendicular direction.

The results shown in Fig. 8–10 can provide some reasons for the failure to determine the permittivity in the z direction, ϵ_3, for the anisotropic material (Boeing) as indicated in Fig. 7. From Fig. 7, the three principal permittivities are: $\epsilon_1 = 3.5 - j5$, $\epsilon_2 = 3.2 - j6$ and ϵ_3 being unstable (not shown). These measured permittivities are in the same order of magnitudes as that used in the examples of Figs. 8–10. In these examples, we observe that if the material thickness is less than 1.75 mm, a change in the conductivity in the z direction causes very small change in the probe input impedance. The thickness of the Boeing material represented in Fig. 7 is only 1.35 mm. Thus, it is difficult to inversely determine ϵ_3 from the measured probe input impedance.

Employing a similar scheme to analyze the anisotropic material of Fig. 6, we first found that three principal permittivities at 10 GHz are approximately equal to $\epsilon_1 = 5.1 - j0.2$, $\epsilon_2 = 5.3 - j0.3$ and $\epsilon_3 = 2.5 - j1.7$. By assuming the same order of magnitudes for the tensor permittivity in the calculation, we can obtain similar results as Fig. 8 and Fig. 9 on the probe input admittance when the material conductivity is varied in the x and y directions, respectively. However, when the material conductivity in the z direction is varied, the theoretical probe input admittance as a function of the material thickness is shown as Fig. 11. We found that when the anisotropic material becomes highly conductive in the direction perpendicular to the waveguide aperture, the effect of the conductance on the probe input admittance becomes significant if the material layer is thicker than about 1.75 mm. Since the thickness of the glass-fiber/epoxy shown in Fig. 6 is 2.8 mm which is thicker than 1.75 mm, we can then inversely determine three principal complex permittivities of the glass-fiber/epoxy without any difficulty.

We have measured only three principal complex permittivities, ϵ_1, ϵ_2, and ϵ_3, in the x, y and z directions. Once

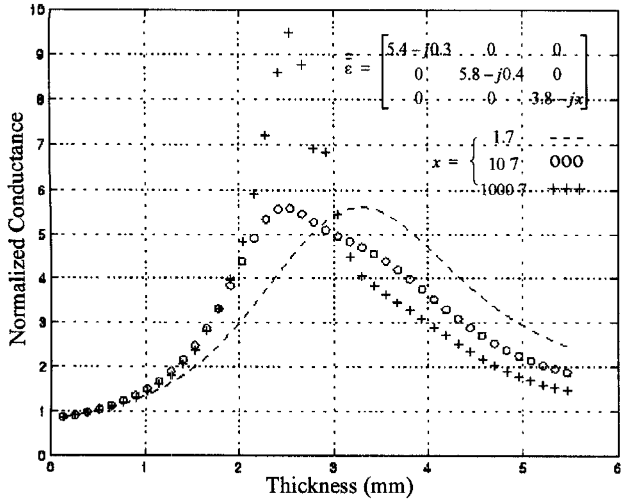

(a)

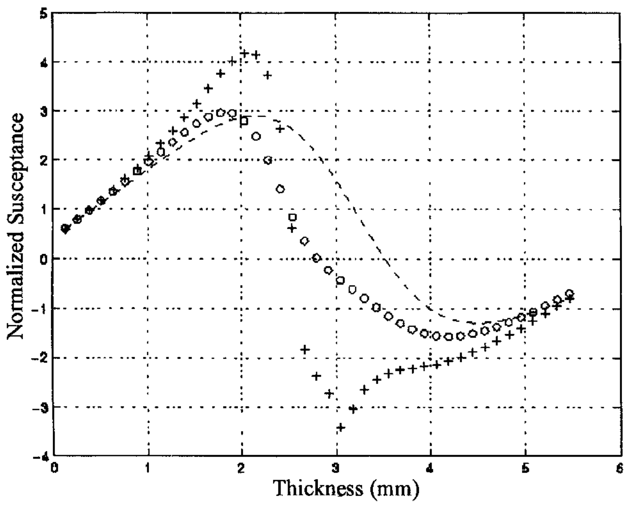

(b)

Fig. 11. Theoretical probe input admittance as a function of the material thickness at 10 GHz when the probe is placed against an anisotropic material layer as shown in Fig. 6 with various conductivities in the z direction.

these principal permittivities are determined, the off-diagonal permittivities, ϵ_{xy}, ϵ_{xz}, ϵ_{yx}, and ϵ_{yz}, can be easily calculated by a simple rotation of the probe orientation angle [17].

VI. Conclusion

This paper presents a technique using a flanged open-ended waveguide probe to nondestructively measure the EM properties of either isotropic or anisotropic materials. The numerical results on the probe input admittances were compared with the existing results published by other workers and they showed a good agreement between them. A series of experiments was conducted on various materials. The EM parameters of the materials were then inversely determined from the measured probe input admittance. The inverse results of some known materials were found to be quite satisfactory. The results on the tensor permittivities of some anisotropic materials were found to be reasonable even though their exact values were not determined before. It was found that to determine the tensor permittivities accurately, specially that in the z direction, the thickness of the anisotropic material sample needs to be greater than some value.

It is believed that the proposed scheme in this paper is capable of simultaneously determining both the complex permittivity ϵ and permeability μ of either isotropic or anisotropic materials with the waveguide probe system. To eliminate the air-gap effect around the probe aperture, an extension of the analysis of the waveguide probe system with a stratified material layer is suggested for a future study to further improve the accuracy of the measurement.

References

[1] E. Tanabe and W. T. Joines, "A nondestructive method for measuring the complex permittivity of dielectric materials at microwave frequencies using an open transmission line resonator," *IEEE Trans. Instrum. Meas.*, vol. IM-25, pp. 222–226, Sept. 1976.

[2] J. R. Mosig *et al.*, "Reflection of an open-ended coaxial line and application to nondestructive measurement of material," *IEEE Trans. Instrum. Meas.*, vol. IM-30, pp. 46–51, Jan. 1981.

[3] M. A. Stuchly and S. S. Stuchly, "Coaxial line reflection method for measuring dielectric properties of biological substances at radio and microwave frequencies—a review," *IEEE Trans. Instrum. Meas.*, vol. IM-29, pp. 176–183, Sept. 1980.

[4] G. B. Gajda and S. S. Stuchly, "Numerical analysis of open-ended coaxial lines," *IEEE Trans. Microwave Theory Tech.*, vol. MTT-31, pp. 380–384, May 1983.

[5] S. Fan, K. Staebell, and D. Misra, "Static analysis of an open-ended coaxial line terminated by layered media," *IEEE Trans. Instrum. Meas.*, vol. 39, pp. 425–437, Apr. 1990.

[6] S. Fan and D. Misra, "A study on the metal-flanged open-ended coaxial line terminating in a conductor-backed dielectric layer," in *1990 IEEE Instrumen. Meas. Technol. Conf. Record*, pp. 43–46.

[7] D. K. Misra *et al.*, "Noninvasive electrical characterization of materials at microwave frequencies using an open-ended coaxial line: Test of an improved calibration technique," *IEEE Trans. Microwave Theory Tech.*, vol. 38, pp. 8–14, Jan. 1990.

[8] Belhadj-Tahar, N. E., A. Fourrier-Lamer, and H. de Chanterac., "Broadband simultaneous measurement of complex permittivity and permeability using a coaxial discontinuity," *IEEE Trans. Microwave Theory Tech.*, vol. 38, pp. 1–7, Jan. 1990.

[9] H. Zheng and C. E. Smith, "Permittivity measurements using a short open-ended coaxial line probe," *IEEE Trans. Microwave Guided Wave Lett.*, vol. 1, no. 11, Nov. 1991.

[10] L. L. Li, N. H. Ismail, L. S. Taylor, and C. C. Davis, "Flanged coaxial microwave probes for measuring thin moisture layers," *IEEE Trans. Biomed. Eng.*, vol. 39, pp. 49–57, Jan. 1992.

[11] B. Chevalier, M. Chatard-Moulin, J. P. Astier, and P. Y. Guillon, "High-temperature complex permittivity measurements of composite materials using an openended waveguide," *J. Electromagn. Waves Applicat.*, vol. 6, no. 9, pp. 1259–1275, 1992.

[12] C. L. Li and K. M. Chen, "Determination of electromagnetic properties of materials using flanged open-ended coaxial probe—full-wave analysis," *IEEE Trans. Instrum. Meas.*, vol. 44, pp. 19–27, Feb. 1995.

[13] M. C. Decreton and F. E. Gardiol, "Simple nondestructive method for the measurement of complex permittivity," *IEEE Trans. Instrum. Meas.*, vol. IM-23, pp. 434–438, Dec. 1974.

[14] M. C. Decreton and M. S. Ramachandraiah, "Nondestructive measurement of complex permittivity for dielectric slabs," *IEEE Trans. Microwave Theory and Tech.*, vol. MTT-23, pp. 1077–1080, Dec. 1975.

[15] J. A. Stratton, *Electromagnetic Theory*. New York: McGraw-Hill, 1941, pp. 392–395.

[16] T. M. Roberts, "Explicit eigenmodes for anisotropic media," *IEEE Trans. Magn.s*, vol. 26, pp. 3064–3071, 1990.

[17] C. W. Chang, "Nondestructive measurements of electromagnetic parameters of anisotropic materials using an open-ended waveguide probe system," Ph.D. dissertation, Dept. Elec. Eng., Michigan State Univ., East Lansing, MI, 1995.

[18] J. Galejs, "Admittance of a waveguide radiating into stratified plasma," *IEEE Trans. Antennas Propagat.*, vol. AP-13, pp. 64–70, Jan. 1965.

[19] R. F. Harrington, *Field Computation by Moment Methods.* New York: Macmillan, 1968.

[20] W. F. Croswell, R. C. Rudduck, and D. M. Hatcher, "The admittance of a rectangular waveguide radiating into a dielectric slab," *IEEE Trans. Antennas Propagat.*, vol. AP-15, pp. 627–633, Sept. 1967.

[21] H. Baudrand, J.-W. Tao, and J. Atechian, "Study of radiating properties of openended rectangular waveguides," *IEEE Trans. Antennas Propagat.*, vol. 36, pp. 1071–1077, Aug. 1988.

[22] E. F. da Silva and M. K. McPhun, "Calibration techniques for one port measurement," *Microwave J.*, pp. 97–100, June 1978.

[23] C. L. Lee, "Measurement of electromagnetic properties of material via coaxial probe systems," Ph.D. dissertation, Dept. Elec. Eng., Michigan State Univ., East Lansing, MI, 1993.

[24] R. L. Johnston, *Numerical Methods-A Software Approach.* New York: Wiley, 1982, ch. 4.

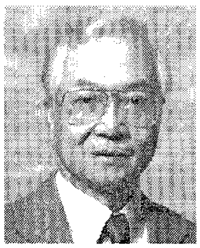

Kun-Mu Chen (F'76) was born in Taipei, Taiwan, on February 3, 1933. He received the B.S. degree in electrical engineering from National Taiwan University in 1955, and M.S. and Ph.D. degrees in applied physics from Harvard University, Cambridge, MA, in 1958 and 1960, respectively.

From 1960 to 1964 he was associated with the Radiation Laboratory, The University of Michigan, Ann Arbor, where he was engaged in the studies of electromagnetics and plasma. Since 1964 he has been with Michigan State University, East Lansing, first as Associate Professor, and from 1967 to 1995 as Professor of Electrical Engineering. In 1995 he became Richard M. Hong Professor of Electrical Engineering. From 1968 to 1973 he was the Director of Electrical Engineering program of the Department of Electrical Engineering and Systems Science. He was a Visiting Professor with Chao-Tung University, Taiwan, in 1962, with National Taiwan University, Taiwan in 1989, and with Tohoku University, Japan in 1989. He has published many papers on electromagnetic radiation and scattering, radar target discrimination and detection, plasma and bioelectromagnetics.

Dr. Chen is a Fellow of AAAS. He received the Distinguished Faculty Award from Michigan State University in 1976, the Withrow Distinguished Scholar Award from the College of Engineering, Michigan State University in 1993, and the Outstanding Achievement Award from Taiwanese American Foundation in 1984.

Chih-Wei Chang (S'94–M'96) was born in Taichung, Taiwan, on August 6, 1962. He received the B.S. degree from Chung-Yuan Christian University, Chung-Li, Taiwan, in 1985, the M.S. degree from University of Missouri-Columbia, Columbia, in 1991, and the Ph.D. degree from Michigan State University, East Lansing, in 1995, all in electrical engineering.

From 1992 to 1995 he was a Research Assistant in the Department of Engineering, Michigan State University, where he worked on the nondestructive measurement techniques for determining the electromagnetic properties of isotropic and anisotropic materials. In 1995 he joined the R&D Department of Taian Electric Co., which is the leading manufacturer of magnetic contactors and circuit breakers in Taiwan, as a Research Engineer, developing the optimized productions with virtual prototyping softwares. His current interests are in theoretical and computational electromagnetics, high frequency, and microwave devices and circuits, and antennas.

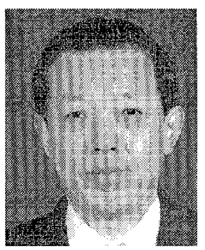

Jian Qian (M'96) was born in 1942 in Jiangsu Province, China. He graduated from Nanjing University in 1964 followed by a graduate program in radio physics, which was interrupted by the Cultural Revolution. He returned to Nanjing University to continue his study in October 1978 and received the M.S. degree in microwave theory and technology in 1981.

From 1968 to 1978, he was with the Nanjing Daqiao Machinery Factory where he was involved in the design of various antennas and transmission line systems for weather radar and satellites receiver, etc. Since then he kept his faculty position in the Microwave Group, Electronic Science, and Engineering Department at the same University. His research interest include the areas of computational electromagnetics, radar scattering, RCS reduction, radar absorbing materials and microwave measurement. From May 1993 to July 1995, he visited Michigan State University as a Research Associate.